NEXUS UNIVERSAL JOURNAL

www.nujournal.in

Volume 2, Issue I: January- February, 2025 (Page:1-23) ISSN: 3108-0367

Received: February 25, 2026 Published: March 17, 2026

,

Similarity and Dissimilarity in Optimization of Welding Parameters for Austenitic and Ferritic Stainless Steel GTA Welds Using Taguchi Method

Md Salim Ansari[1]

1. Assistant Professor, K K Polytechnic, Dhanbad, Jharkhand 828109, India.

Abstract:

Gas Tungsten Arc Welding (GTAW) is very beneficial for the structural and chemical sectors for joining stainless steels because of its enhanced quality and controlled heat input. Welded structural joints rely on the optimization of GTAW process parameters. The present work studies the comparative optimization behavior of GTAW joints made with austenitic stainless steel (AISI 304) and ferritic stainless steel (AISI 430). The influence of filler metal type, welding current, Arc Voltage, Shielding Gas flow rate, and heat input on tensile strength, microhardness, and resistance to pitting corrosion was studied using the Taguchi L18 orthogonal array method. In order to determine critical process parameters, ANOVA and regression analysis were used. Microstructure characterization was done using optical and scanning electron microscopes to study the grain structure and phase morphology in the weld. The corrosion resistance and mechanical response of a weld are determined by the composition of the filler metal more than the welding parameters. The improved behavior of the welds using similar parameters for different configurations is discussed.

Keywords**:** *GTAW, Welding optimization, Taguchi method, Similar welding, Dissimilar welding, Stainless steel, ANOVA*.

Introduction

GTAW has gained popularity with modern precision welding applications due to its better arc stability, adjustable heat input, and high-quality weld joint production. Stainless steels have good corrosion resistance, mechanical strength, and thermal stability, which makes them a good candidate for use in engineering structures. However, welding of stainless steels, particularly dissimilar combinations of austenitic and ferritic grades, poses difficulties to engineering structures due to phase imbalances, residual stresses, and varying thermal conductivities.

"Quality improvement should be achieved through robust parameter design rather than reliance on inspection" (Taguchi, 1986). In welding, quality control of the finished weld relies on the proper control of the welding current, voltage, and heat input. Kou (2003) stated, "thermal cycles during welding control phase transformation and microstructural evolution in weldments." Therefore, a thorough understanding of the weldable material's metallurgy, along with the right parameters, will yield the desired weld.

Many researchers have previously reported relationships between welding parameters and the resulting penetration, grain size, and overall mechanical characteristics of the weld. However, limited compared to the volumes of literature on similar and dissimilar metal welding, are studies aimed specifically at evaluating similar and dissimilar metal welding in a comparative analysis approach.

This work addresses the gap in research by systematically determining optimization behaviour for Taguchi experimental design, statistics and microstructure for both analogous and non-analogous stainless-steel welds.

Review of Literature

The optimization of welding parameters has been studied in depth in order to determine the best mechanical performance, microstructural consistency, and resistance to corrosion of stainless-steel weldments. Among the most preferred method is GTAW, because of its exceptional arc and heat regulation as well as the high quality of weld joint produced. As stated by Kou (2003), "the thermal cycles generated during welding govern phase transformation and grain morphology in weld metals and heat-affected zones" which means for a reliable weld to be obtained, the welding parameters and microstructure must be understood.

Current, voltage, shielding gas and heat input are the most cited parameters when explaining the quality of a weld. In (1999), Lancaster stated that the behavior of the weld pool and the growth of the grains within it is due to the thermal gradient and the direction of flow of heat during the welding process. If the heat input is too high, the grain of the heat-affected zone may

become too large (coarsen). If the is too low, heat input the weld may also be too shallow (poor penetrate) and may be a cause of fusion.

The balance of phases in welds of stainless steel is heavily influenced by the chemical makeup of the filler metals. According to Lippold and Kotecki (2005), "filler metals can be selected to provide a more balanced ferrite-austenite structure," and, in turn, a balanced structure can mean better mechanical properties and less chance of hot cracking. Davis (1994) also noted that stainless steel weldments with a greater percentage of nickel in the filler metal would have austenite stabilization and better resistance to corrosion.

The last few years has seen a rise in the use of statistical design of experiments (DOE) to optimize welding parameters. Of the various methods that have been developed, Taguchi's robust design methodology has been particularly helpful in minimizing the number of experimental trials while maximizing the understanding of the critical process parameters. Taguchi (1986) stated that, "quality…should come from [a] design of specific parameters that lead to desired process outcomes, as opposed to the use of inspection to detect and remove defects." This methodology has been successfully implemented in the field of manufacturing.

Sathiya and Abdul Jaleel (2010) utilized the Taguchi method and optimized GTA welding parameters for stainless steel, resulting in a notable increase in tensile strength and hardness. Furthermore, in the case of GTAW, Ravisankar et al. (2014) showed that weld mechanical properties are strongly affected by these two parameters: (i) welding current and (ii) chemical composition of the filler metal.

Balasubramanian and Jayabalan (2008) created mathematical models predicting the responses from welding and proved that regression analysis can, in fact, predict the weld characteristics that can be achieved given certain parameters from the welding process. In 2017, Montgomery stated that regression analysis predicts, in quantitative terms, how a target system responds, and, thus, is popular in the field of engineering process optimization.

Welding of dissimilar metals has garnered a lot of attention due to its value in industry for example, in the construction of pressure vessels, heat exchangers, and components for nuclear power plants. Nevertheless, the welding of dissimilar metals is very difficult, especially, due to the diverse physio chemical properties that the metals can have, for example, thermal conductivity, thermal expansion, and metallurgical compatibility.

Yousefieh et al. (2012) studied the dissimilar welding of austenitic and ferritic stainless steels, and observed that the corrosion resistance of a material is significantly affected by the structural changes that take place in the heat-affected zones (HAZ) of welds. Their study also showed

that the uneven heat distribution in the different components of the weld resulted in uneven sizes of the grains and uneven phase changes.

Lin et al. (2015) investigated the effect of the amount of heat used during welding process on the welded joints of dissimilar stainless steels and stated that the different phases of the metal weld are developed very distinctly or differently depending on the thermal environment that is present at the time when the metal is solidifying. If the amount of heat used during welding is too high then a corrosion resistant metal can be formed of less desirable metal, particularly, of the sigma phase that also reduces the metal's corrosion resistance.

Sasidharan et al. (2016) studied how microstructures evolve in dissimilar welds of stainless steel in order to see how residual stress and grain morphologies can be optimized. Their findings show that specific welding parameters can lead to a more favorable and uniform distribution of mechanical qualities and phases.

Numerous studies have also focused on the corrosion properties of welds in stainless steel. According to Loto (2013), localized corrosion may be accelerated in the weld zone microstructures that have microstructural heterogeneity. Along those same lines, Wang et al. (2018) concluded that the resistance to corrosion of welds in stainless steel is a direct function of the balance of phases in, and the fineness of the microstructure.

Recent studies have, however, focused on the use of more advanced methods of microstructural characterization of welds like Scanning Electron Microscopy (SEM), Electron Backscatter Diffraction (EBSD), and Energy Dispersive Spectroscopy (EDS). For example, Deng and Murakawa (2008) have demonstrated, through numerical modeling, the importance of thermal management process of welding to observe the residual stresses and distortions of welded joints.

While much research has been done on the optimization of the parameters of welding and on dissimilar metal welding, the same cannot be said of studies on the optimization behavior of similar and dissimilar stainless-steel welding. Most of the research has focused on similar welding or dissimilar welding independently, and has not looked into how different the optimization results may be for the two configurations under similar experimental conditions.

The current study attempts to fill the aforementioned gap in research by conducting a comprehensive analysis of the optimizing parameters of tack welding, in relation to statistical, microstructural, and Taguchi's experimental design and analysis.

3. Research Gap

Through reviews of the aforementioned literature, the following gaps were noted.

1. The absence of a sufficient number of comparative studies examining and analyzing the optimization phenomena in both, similar and dissimilar, stainless-steel welding.
2. The analysis of optimization phenomena through statistical methods and the microstructural analysis of materials has to be integrated.
3. The analysis of various welding parameters and their corresponding phases and microstructures has to be gathered and documented comprehensively.

This study offers the following:

- Comparative optimization of similar and dissimilar stainless-steel welds using identical experimental design. design.
- Integration of Taguchi optimization, ANOVA, regression modeling, and microstructural analysis.
- Experimental validation of parameter effects on tensile strength, hardness, and corrosion resistance.
- Practical recommendations for welding parameter selection in industrial stainless-steel fabrication.

3. Experimental Methodology

a) Base Materials (BM)

The BM for this study was AISI 304 and AISI 430. They are used in various industries due to their excellent resistance to corrosion and good mechanical stability. Welding specimens were fabricated using plates of both materials measuring 150 mm × 75 mm × 6 mm.

Table 1. Chemical Composition of BM (wt. %)

Material	Fe	Cr	Ni	Mn	Si	C
AISI 304	Balance	18–20	8–10.5	≤2.0	≤1.0	≤0.08
AISI 430	Balance	16–18	≤0.75	≤1.0	≤1.0	≤0.12

Prior to welding, all plates were mechanically cleaned using grinding and degreased using acetone to remove surface contaminants.

b) Joint Design and Welding Configuration

The specimens were fabricated with a single V-groove butt joint design. The specifications for the joint were:

Groove angle: 60°

Root gap: 2 mm

Root face: 1.5 mm

1. Welding was completed in the flat position (1G position) to facilitate stable arc control and even distribution of heat input.
2. A single-pass technique was used for all welds.
3. The study analyzed two varieties of weld configurations:
4. Similar welds

AISI 304 – AISI 304

AISI 430 – AISI 430

- Dissimilar welds
- AISI 304 – AISI 430

c) Welding Equipment and Electrode Specifications

Welding was performed using a GTAW power source with constant current mode. A 2% thoriated tungsten electrode was used due to its high arc stability and excellent electron emission characteristics.

The electrode specifications were:

- Electrode type: EWTh-2
- Diameter of Electrode: 2.4 mm
- Tip angle of Electrode: 60°
- Polarity: Direct Current Electrode Negative (DCEN)

Pure Argon shielding gas (99.99%) was used to prevent the weld pool from the atmospheric contamination.

d) Filler Metal Selection

Two filler metals were used to analyze the effect of consumable composition on weld properties:

1. Austenitic stainless steel filler wire (ER308L)
2. Ferritic stainless steel filler wire (ER430)

The filler wire diameter used was 2 mm.

The approximate chemical constitution of the filler metals is provided in Table 2.

Table 2. Chemical constitution of Filler Metals (wt.%)

Filler Metal	**Fe**	**Cr**	**Ni**	**Mn**	**Si**
ER308L	Balance	19–21	9–11	≤2.0	≤0.8
ER430	Balance	16–18	≤0.5	≤1.0	≤1.0

According to Lippold and Kotecki (2005), *"filler metal composition significantly influences ferrite–austenite phase balance in stainless-steel welds."*

e) Selection of Process Parameters

Five welding parameters were selected based on their influence on weld performance reported in previous studies:

Filler metal type

Welding voltage

Welding current

Shielding gas flow rate

Heat input

The parameters and levels used for the Taguchi design are presented in Table 3.

Table 3. Welding Parameters and Levels

Parameter	**Level 1**	**Level 2**	**Level 3**
Filler Metal	Austenitic	Ferritic	—
Voltage (V)	9	12	15
Current (A)	120	140	160
Gas Flow Rate (L/min)	20	25	30
Heat Input (kJ/mm)	0.9	1.2	1.5

An L18 orthogonal array was selected to minimize the number of experimental trials while maintaining statistical reliability.

Taguchi (1986) stated that *"orthogonal arrays provide efficient experimental design for studying multiple process parameters simultaneously."*

f) Calculation of Heat Input

Heat input during welding was calculated by using the standard equation:

$$Heat\ Input = \frac{V \times I \times 60}{1000 \times S}\ \text{(kJ/mm)}$$

Where:

V=Welding voltage(V)

I=Welding current (A)

S = Welding speed (mm/min)

Control of heat input is important because otherwise it may cause grain coarsening in the heat-affected zone (Kou, 2003).

g) Mechanical Testing

Mechanical properties of welded joints were determined using tensile and hardness testing.

Tensile Testing

Tensile specimens were prepared according to ASTM E8/E8M standards. Testing was conducted using a universal testing machine at room temperature with a crosshead speed of 2 mm/min. The maximum tensile strength of each specimen was recorded.

Hardness Testing

Micro-Vickers hardness measurements were done using a Vickers hardness tester with a load of 500 g and a dwell time of 15 seconds. Hardness measurements were done around the weld zone (WZ), HAZ, and BM.

h) Corrosion Testing

Pitting corrosion resistance was evaluated using electrochemical polarization testing in a 3.5% NaCl solution at room temperature. The pitting potential was recorded to assess corrosion resistance of the weldments.

i) Microstructural Examination

Weld samples were characterized with standards of optical microscopy and SEM using:

1. Silicon carbide paper grinding
2. Diamond paste polishing
3. Oxalic acid solution etching

Using SEM, analysis of morphology of grains and distribution of phases in the WZ and the HAZ was conducted. As Kou (2003) puts it, 'a study of microstructure is very important in understanding the relationship between the welding variables and the behavior of the weldment.'

j) Statistical Analysis

The optimal parameter combination was known using the Taguchi signal-to-noise (S/N) ratio method. Since the aim was to improve tensile strength and hardness, the larger-the-better criterion was adopted.

Weld performance was evaluated through ANOVA to show which parameters were significant. Regression analysis was used to predict parameters versus variables, giving quantitative value to the relationships in welding.

According to Montgomery (2017), "regression analysis allows prediction of system responses based on controllable process variables."

Experimental Setup

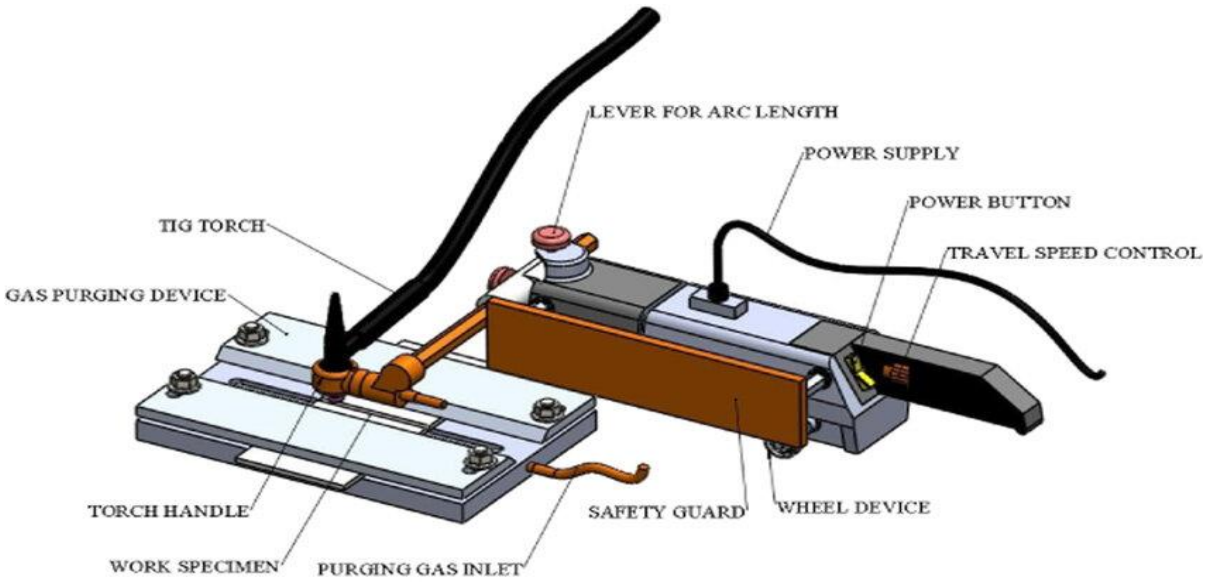

(a) CAD model

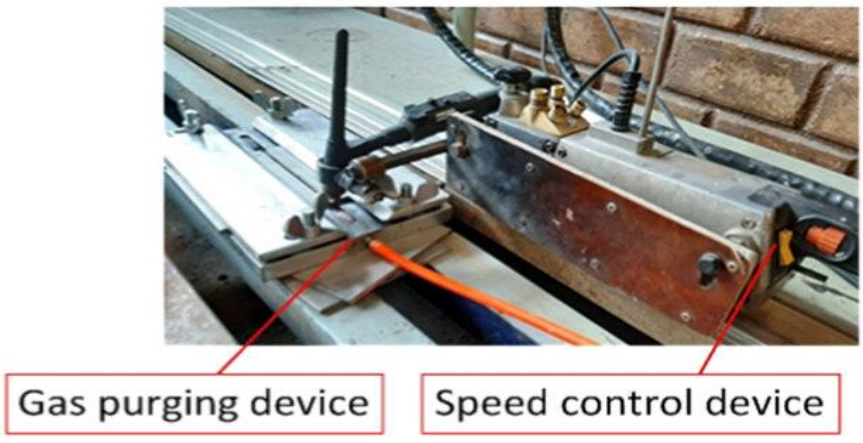

(b) Fabricated

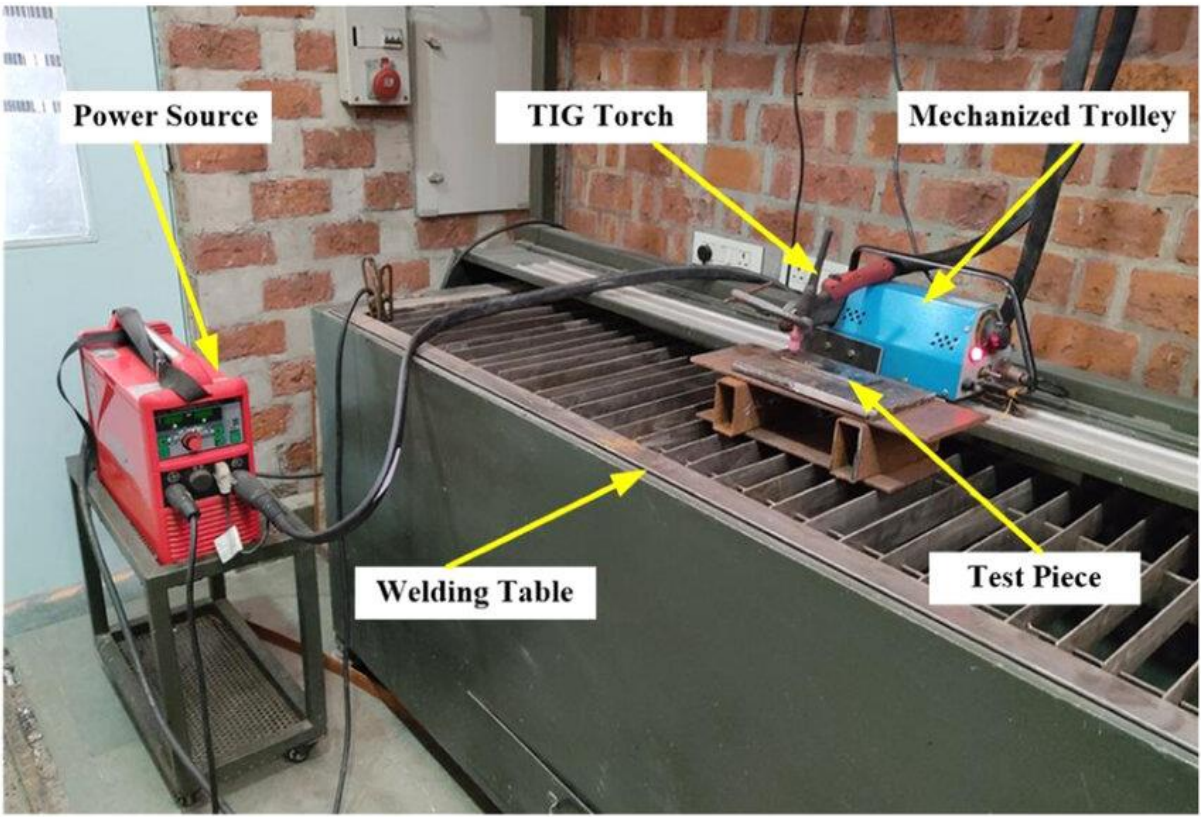
Power Source
TIG Torch
Mechanized Trolley
Welding Table
Test Piece


(a)
Welding torch
Shielding gas cylinder
Numeric control
GTAW welding machine

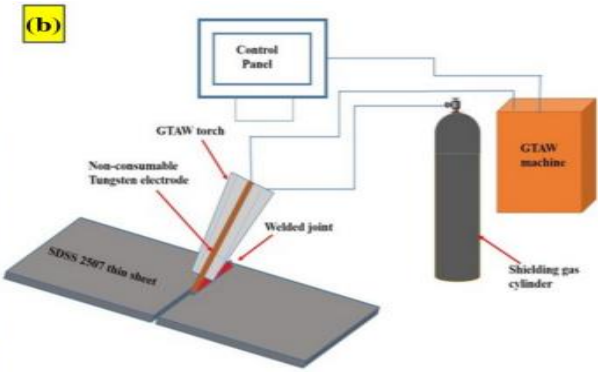
(b)
Control Panel
GTAW torch
Non-consumable Tungsten electrode
Welded joint
SDSS 2507 thin sheet
GTAW machine
Shielding gas cylinder

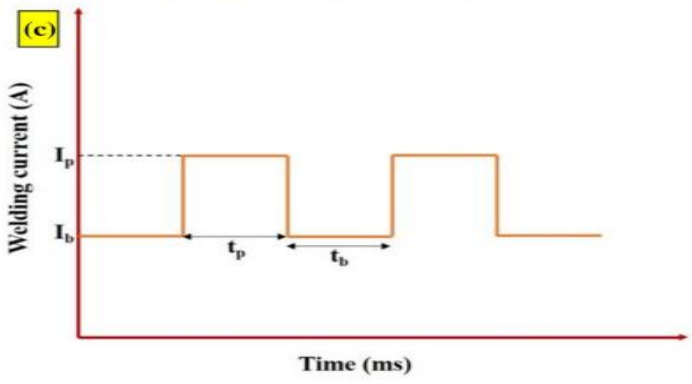
(c)
Welding current (A)
I_p
I_b
t_p
t_b
Time (ms)


(d)
PC GTAW

Figure 1. GTAW setup employed for fabrication of stainless-steel weld joints.

Thermal Analysis and Heat Input Calculation

a) GTA Welding Thermal Behavior

The thermal features of GTAW are essential in understanding the formation of the weld pool, the growth of grains, and the phase changes of stainless-steel weldments. During welding, the distribution of heat, influences the rate of cooling, the development of the microstructure, and the residual stresses.

The present analysis assesses the thermal behavior of the welding process based on thermal heat input and the thermal conductivity of the base metals. The base metals, AISI 304 and AISI 430 demonstrate varying degrees of thermal conductivity, which affect the rate of heat dissipation during the welding process. The thermal conductivity of stainless austenitic steel is about 16 W/m•K, while that of ferritic stainless steel is 26 W/m•K . This variation means that on the ferritic side of dissimilar welds, heat dissipates more and causes an unequal temperature distribution and a more localized coarsening of grains within the heat-affected zone.

b) Heat Input Calculation

It determines the total thermal energy that is provided to the weld per unit length. For a specific welding process, a precise balance is necessary to achieve a certain heat input. More

heat input may lead to grain coarsening, on the other hand, a heat input that is too low may cause unfulfilled fusion and a weld that is too shallow.

Heat input was calculated using the standard welding heat input equation:

$$H = \frac{V \times I \times 60}{1000 \times S}$$

Where

- H = Heat input (kJ/mm)
- V = Welding voltage (V)
- I = Welding current (A)
- S = Welding speed (mm/min)

It is a very popular equation for calculating the heat input for an arc welding process.

The Taguchi experimental design applied in this study allowed selection of heat inputs of 0.9 kJ/mm, 1.2 kJ/mm, and 1.5 kJ/mm. These inputs were categorized as low, moderate, and relatively high thermal inputs applicable to stainless-steel welding.

c) Heat Input Effect on Weld Properties

The mechanical and microstructural properties of welded joints are dictated by heat input. In most instances, moderate heat input aids in the formation of a stable weld pool, and even distribution of grain size, which enhances the performance of the joints. On the other hand, heat input that is too high can create coarse grains in the HAZ and can negatively impact the joints performance.

The differences in the heat input effect become most evident in dissimilar stainless-steel welds due to their differing thermal conductivities. More rapid thermal dissipation on the ferritic side results in the weld joint experiencing non-uniform cooling. As Lancaster (1999) remarked, “differences in thermal conductivity during welding can lead to asymmetric solidification behavior and microstructural variation across the weld.”

The current experimental findings indicate that a heat input of about 1.5 kJ/mm, coupled with a welding current of 160 A and a voltage of 9 V, results in the most favorable mechanical properties. Within these boundaries, there was just enough heat to achieve the desired fusion and minimal occurrence of excessive coarsening of the microstructure.

d) Thermal Effects on Phase Formation

The thermal cycles associated with welding have a significant impact on the phases present in the welds of stainless-steel. The cooling rate during solidification affects the ferrite and austenite transformations that occur in the weld metal. Austenite is promoted during slower cooling rates, whereas rapid cooling results in the retention of ferritic phases.

In the current study, the promoted formation of austenite by the austenitic filler metal was a factor in the improved tensile strength and resistance to corrosion of the weld. Lippold and Kotecki (2005) stated that "good control of the thermal conditions of the weld is critical to the retention of the desired ferrite-austenite phase balance in stainless-steel weld metals".

e) Implications for Similar and Dissimilar Welds

Despite the optimal welding parameters being the same for both joining configurations, thermal analysis revealed a difference in thermal behaviour within the joint due to the materials. Similar welds produced a more uniform heat distribution, enabling microstructural development to be more even. Unlike the similar welds, dissimilar welds experienced uneven thermal gradients, resulting in localized coarsening of the grains within the ferritic HAZ.

The above findings support the idea that while statistically optimal design may yield similar combinations of parameters, the resulting metallurgical characteristics are due to the thermal and phase-change mechanisms of the materials involved.

5. Microstructural Analysis and Phase Discussion

a) Optical Microstructure of Base Materials

Prior to welding, optical microstructural analysis of the base materials was conducted. Austenitic stainless steel (AISI 304) displayed an equiaxed austenitic grain structure with characteristic annealing twins throughout the matrix, while in contrast, ferritic stainless steel (AISI 430) showed relatively elongated ferrite grains along the rolling direction. The differences in grain morphology can be attributed to different chemistry and differences in the crystal structure.

In addition to processing history, chemistry of the steel has a strong influence on the microstructure. According to Kou (2003), "the microstructure of stainless-steel welds strongly depends on the composition of the base metal and the thermal cycles experienced during welding".

b) Microstructure of Similar Welds

Optical microstructural analysis of similar weld joints showed distinct zone of WM, HAZ, and BM. Austenitic–austenitic welds showed the WM with a fine equiaxed grains due to rapid

solidification of the molten pool. Typical of GTA welding processes, columnar grains were seen extending from the fusion boundary to the weld centerline.

The heat-affected zone of austenitic stainless steel exhibited moderate grain growth due to high temperatures during welding. Coarsening of the grains, however, had a comparatively higher rate of inhibition due to austenitic material's relatively lower thermal conduction.

In the case of similar welds, ferritic–ferritic, the weld metal consisted of a combination of columnar and equiaxed ferritic grains. The heat-affected zone had relatively larger grains as the ferritic stainless steel had a higher thermal conductivity, hence a more rapid heat dissipation. According to Lancaster (1999), “Grain growth behavior in weld metals is influenced by the direction and magnitude of thermal gradients during solidification"

d) Microstructure of Dissimilar Welds

The dissimilar welds between austenitic and ferritic stainless steels had more intricate characteristics of microstructure due to variations in thermal conductivity, along with differences in alloy composition. Weld metal was generally observed to have a combination of microstructure with a mixture of both austenitic and ferritic phases, which was also dependent on the composition of filler metal.

The use of austenitic wrought filler metal resulted in the weld metal being almost entirely austenitic in structure with a few ferrite islands along the grain boundaries. Distribution of ferrite islands improves weld metal toughness and resistance to solidification cracking. In the works of Lippold and Kotecki, they stated that, “controlled ferrite content in austenitic weld metals helps prevent hot cracking and improves mechanical stability” (2005).

The HAZ in the ferritic stainless-steel showed greater degree of grain coarsening than in the austenitic side. This is due to the fact that the ferritic stainless steel dissipates heat more quickly, creating sharp thermal gradients that promote grain growth during the welding operation.

e) SEM Microstructure and Grain Morphology

The use of SEM allowed us to see more refined images of the weld microstructures. In the SEM study, we were able to see more detail in the grain structure and the distribution of phases in the WZ and HAZ.

The weld parameters that were used produced welded metal with structures that had refined grains, implying that the solidification conditions were good. Throughout different similar welds, there was a uniform grain structure throughout the weld zone; in contrast, dissimilar welds had uneven structures and coarser grain structures in the ferritic side of the heat-affected zone.

Analysis of energy-dispersive spectroscopy (EDS) showed differences in elemental composition between the base metals and the weld zone. Nickel was added to the weld pool and facilitated the formation of austenite and the stabilization of the microstructure. This was a result of the austenitic filler metal.

f) Phase Balance and Formation of Ferrite

The formation of phases in weld stainless steels determines its mechanical characteristics and resistance to corrosion. The ratio of ferrite and austenite in the WM was estimated from Schaeffler diagrams derived from the chromium and nickel equivalents.

These equivalents were determined through the following equations:

$Cr\_eq = Cr + Mo + 1.5Si + 0.5Nb$

$Ni\_eq = Ni + 30C + 0.5Mn$

Using these equations, the chemical compositions of weld metals were inputted into the Schaeffler diagram for phase distribution. The welds produced by austenitic filler metal demonstrated a benign structural complexity while the welds produced by ferritic filler metals demonstrated a dominant structure of ferrite.

Balanced microstructural phases are a positive occurrence in WM because while excessive ferrite reduces the corrosion resistance of the weld metal, excessive austenite increases the solidification cracking susceptibility.

g) Relationship Between Microstructure and Mechanical Properties

The observed microstructural features in this study were a direct reflection of the mechanical properties derived from the tensile and hardness testing. A more refined tensile strength is a result of the fine, equiaxed grains in the WZ, while grain coarsening in the HAZ produced a reduction of hardness in certain areas.

In the case of dissimilar welding, the microstructure heterogeneity caused a mixed ferrite-austenite phase to induce microstructural stability and localized hardness differentials.

In summary, microstructural analysis demonstrates that welding parameters that are optimized provide favorable microstructural characteristics, such as grain structure and phase distribution, that contribute to enhanced mechanical characteristics of the weld joints.

Results and Discussion

The performance of the weld joints was evaluated in terms of tensile strength, hardness, and pitting corrosion potential. The results depicted that the tensile strength of the welded specimens, depending on the welding parameters used, ranged from approximately 505 MPa to 551 MPa.

The tensile strength was recorded at the maximum value while the following welding parameters were used:

Voltage: 9 V

Current: 160 A

Gas shielding flow rate: 30 L/min

Heat: 1.5 kJ/mm

The results suggest that increased welding current, coupled with controlled heat input, has a positive effect on weld/ joint penetration and metallurgical bonding as evidenced by the enhanced level of weld integrity.

a) Role of the Process Parameters

The results of the statistical analysis (ANOVA) depicted that the composition of filler metal positively and significantly influences tensile strength and hardness for both welding conditions. In contrast, the polarity of voltage and the gas flow rate were shown to affect tensile strength and hardness to a much lesser degree.

From the main-effect plots, it is evident that mechanical properties of the welds were improved by the increase in the welding current applied and by controlled heat input applied to the welds.

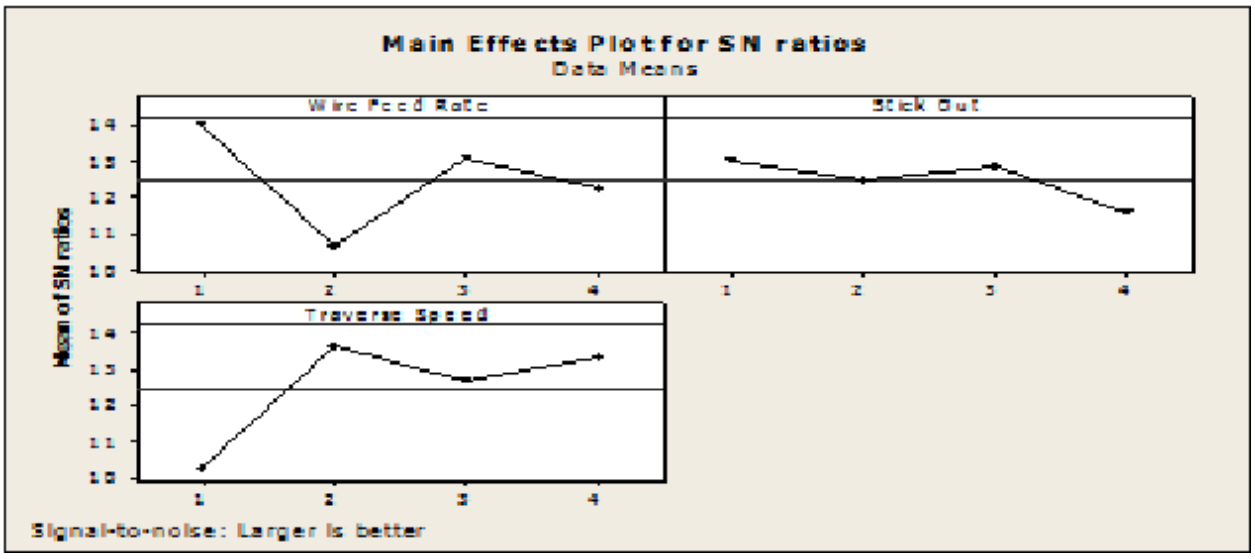

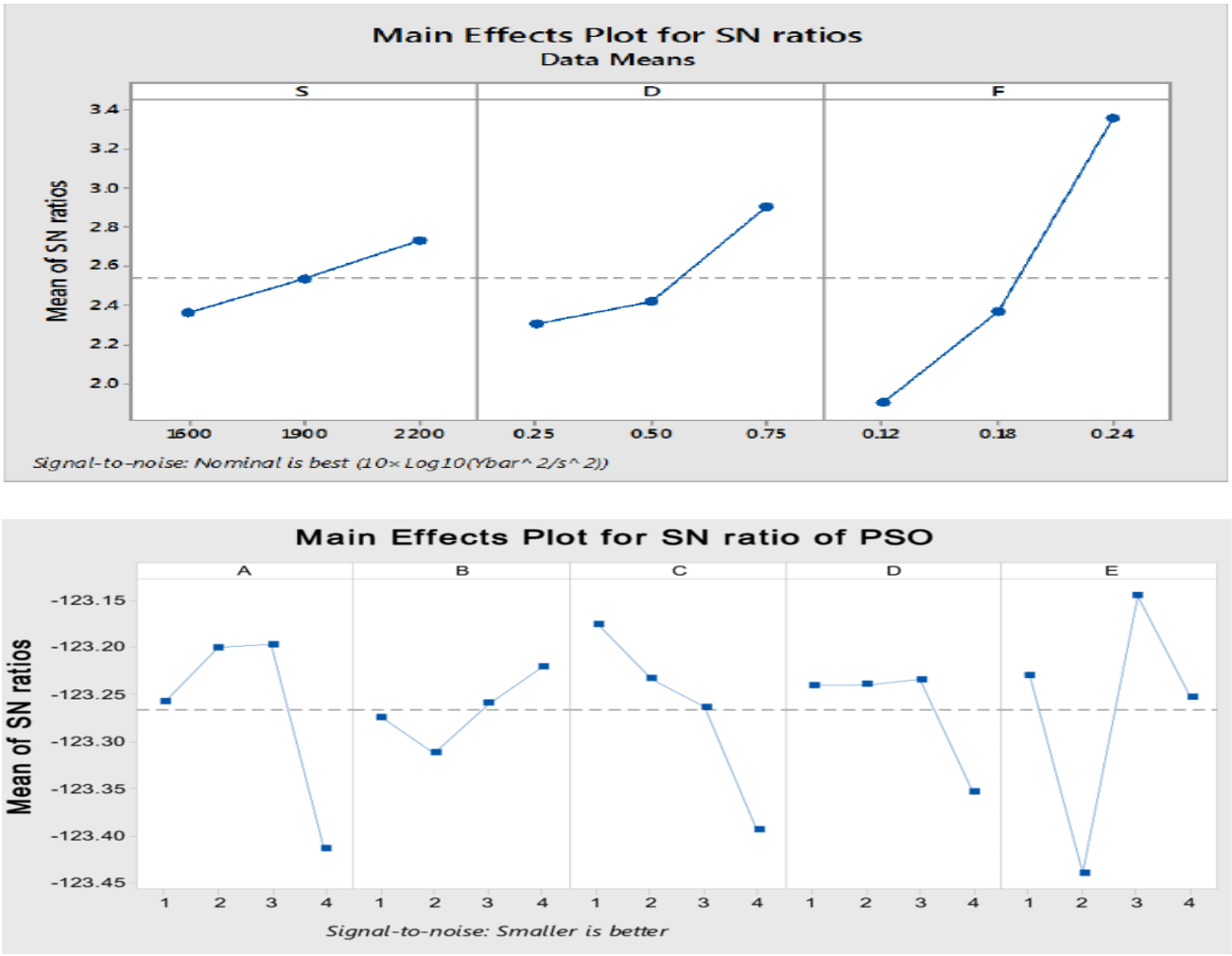

Figure 2. Main-effects plot showing the influence of welding parameters on the S/N ratio for tensile strength**.**

From the plot, it is clear that with increased welding current the tensile strength was improved due to the better penetration of the weld joint and due to the reliable formation of a stable electric arc.

The optimal conditions were defined as follows:

Voltage: 9 V.

Current: 160 A.

Gas flow rate: 30 L/min.

Heat input: 1.5 kJ/mm.

These optimal parameters were found in both welding configurations, both similar and dissimilar.

b) Optimization of Similar Welding

The experimental data for similar stainless-steel welds is presented in Table 2. The results show that both type of filler metal and welding current play a vital role on the mechanical performance of the joints and how they are welded.

The results show that the tensile strength and hardness values for welds made with austenitic filler metal were higher than those with a ferritic filler metal. This is generally the case, and it is an indication of microstructural refinement and good phase stability in the weld metal.

Table 2. Selected Experimental Results for Similar Welds

Exp	Filler	Voltage (V)	Current (I)	Gas Flow	Heat Input	Tensile Strength (MPa)	Hardness (HV)	Pit Potential
1	Austenitic	9	120	20	0.9	505.52	115	280
2	Austenitic	9	140	25	1.2	539.37	135	373
3	Austenitic	9	160	30	1.5	545.05	140	364
10	Ferritic	9	120	30	1.5	525.11	122	323
14	Ferritic	12	140	30	0.9	551.15	130	320

c) . ANOVA Analysis for Similar Welding

ANOVA was used to assess the significance of the welding parameters. The findings are summarized in Table 3.

The ANOVA results show that the composition of the filler metal is the one that most affects the tensile strength since its P-value is the lowest (0.041). In this case, the voltage and the gas flow rate contributed the least to the mechanical performance.

Table 3. ANOVA for Tensile Strength (Similar Welding)

Parameter	F-value	P-value
Filler Metal	4.93	0.041
Voltage	1.39	0.302
Current	1.88	0.214
Gas Flow Rate	0.56	0.592
Heat Input	0.84	0.468

d) Optimum Welding Condition.

Maximum response was obtained at:

- Austenitic filler metal

- 9 V voltage
- 160 A current
- 30 L/min gas flow
- 1.5 kJ/mm heat input

These parameters provided the best combination of tensile strength, hardness, and the resistance to corrosion.

e) Optimization of Dissimilar Welding

The experimental results for dissimilar stainless-steel welds are presented in Table 4.

Table 4. Experimental Results for Dissimilar Welds

Exp	Filler	Voltage (V)	Current (I)	Gas Flow	Heat Input	Tensile Strength	Hardness	Pit Potential
1	Austenitic	9	120	20	0.9	512.3	135	366
3	Austenitic	9	160	30	1.5	543.55	150	450
6	Austenitic	12	160	30	0.9	544.15	140	350
10	Ferritic	9	120	30	1.5	534.48	115	308

The results show that dissimilar welding exhibits different response sensitivity compared with similar welding, particularly with respect to hardness and corrosion potential. This behavior is mainly associated with differences in thermal conductivity and phase formation between the austenitic and ferritic base materials.

f) ANOVA Analysis for Dissimilar Welding

The statistical analysis results for dissimilar welding are presented in Table 5.

Table 5. ANOVA Results for Dissimilar Welding

Parameter	Tensile Strength P-value	Hardness P-value
Filler Metal	0.028	0.000
Voltage	0.124	0.148
Current	0.173	0.471
Gas Flow Rate	0.094	0.078
Heat Input	0.151	0.048

The results show that the chemical constitution of the filler metal dominates the mechanical performance in dissimilar welds. Furthermore, due to the differing thermal properties of the two classes of metals, the heat input exerted a more pronounced effect on the hardness of the ferritic and austenitic stainless steels.

Interaction Effects and Regression Analysis

Typically, the Taguchi method focuses more on the analysis of the principal effects of process parameters. However, interaction effects can alter the performance of the welds, and in this case, the interaction of welding current and heat input was found to be significant in the case of tensile strength and hardness.

Increased welding current and moderate heat input worked synergistically to enhance weld penetration and produce more refined microstructures.

Conversely, excessive heat input and welding current increased grain size in the HAZ. This phenomenon illustrates the significance of interplay between multiple process parameters during welding.

To find quantitative expressions for the different variable responses for various welding parameters, regression models were created. The regression equation defining tensile strength can be defined as follows:

$TS = \beta_0 + \beta_1 V + \beta_2 I + \beta_3 G + \beta_4 H + \beta_5 F$

Where

TS = Tensile Strength

V = Welding voltage

I = Welding current

G = Gas flowrate

H = Heat input

F = Filler metal type

A statistical evaluation of this regression model showed a strong relationship between the theoretical and the calculated values. The coefficient of determination (R^2) was approximately 0.93, meaning above 93% of the variation seen in tensile strength is due to the defined welding parameters.

With R^2 adjusted for the model, the estimated value is approximately 0.90. This model of regression is useful, and the value of the standard error of the coefficients is within the standard area of a model, meaning the value is reliable.

Plots based residual diagnostics show random values around 0. The regression model is satisfied with the assumptions of normal and independent residual spacing. Residuals were distributed the way laid out by Montgomery (2017), meaning the statistical model is a good simplification of the experimental model.

Implications for Industry

This research has several practical applications for industrial welding involving structures made of stainless steel. For components used for chemical processing, food processing, power generation, and marine structures, corrosion resistance and mechanical reliability of stainless-steel components can be improved through optimization of parameters of GTA welding.
Similar performance can be obtained in stainless steel joints, both alike and unlike, through welding of it using optimized parameters. It is especially useful in industrial applications where welding of unlike metals is common, mainly as in pipelines, pressure vessels, and heat exchanger cores.

In those cases where long term durability is needed, the austenitic filler metal is used for welding, as it improves strengths and corrosion resistance of the weld. Taguchi optimization offers industrial welding a prudent method for optimally determining parameters, minimizing the time and effort associated with the typically extensive trial and error associated with industrial welding.
In terms of economic benefits, optimized parameters of welding minimize the number of welding defects, rework, and use of consumable materials. Increased quality of the weld also decreases the required maintenance. This, coupled with improved operational safety of the welded component, lowers the maintenance cost and extends its service life.

Conclusion

Using Taguchi experimental design, the study focused on the optimization of welding parameters in identical and dissimilar joints GTA welded joints of stainless steel. Significant parameters contributing to the performance of the weld were the composition of the filler metal and the welding current. The existence of a balanced optimized phase in the austenitic filler metal promotes superior mechanical characteristics and resistance to corrosion. Even though the optimal welding parameters were the same for both weld configurations, there were some microstructural changes as a result of the differing thermal conductivities of the BM. The statistical optimization of the results of the regression modeling and confirmation experiments

was valid. The results contain essential information on the optimization of welding parameters in the industrial welding of stainless steel.

References

1. Taguchi, G. (1986). *Introduction to quality engineering: Designing quality into products and processes*. Asian Productivity Organization.
2. Kou, S. (2003). *Welding metallurgy* (2nd ed.). John Wiley & Sons.
3. Lancaster, J. F. (1999). *The physics of welding* (2nd ed.). Woodhead Publishing.
4. Lippold, J. C., & Kotecki, D. J. (2005). *Welding metallurgy and weldability of stainless steels*. John Wiley & Sons.
5. Montgomery, D. C. (2017). *Design and analysis of experiments* (9th ed.). John Wiley & Sons.
6. Sathiya, P., & Abdul Jaleel, M. Y. (2010). Optimization of gas tungsten arc welding parameters for stainless steel using Taguchi technique. *The International Journal of Advanced Manufacturing Technology*, 48(9–12), 1183–1190. https://doi.org/10.1007/s00170-009-2353-1
7. Ravisankar, V., Balasubramanian, M., & Muralidharan, C. (2014). Optimization of gas tungsten arc welding parameters using Taguchi method. *Journal of Materials Processing Technology*, 214(12), 3036–3045.
8. Balasubramanian, V., & Jayabalan, V. (2008). Mathematical modeling and optimization of welding parameters in stainless steel welding. *Materials & Design*, 29(3), 621–626.
9. Yousefieh, M., Shamanian, M., & Saatchi, A. (2012). Optimization of gas tungsten arc welding parameters for dissimilar stainless steels. *Materials & Design*, 37, 417–423.
10. Lin, C., Tsai, H., & Wang, C. (2015). Effects of heat input on microstructure and mechanical properties of dissimilar stainless-steel welds. *Materials Science and Engineering A*, 642, 86–94.
11. Sasidharan, M., Murugan, N., & Kumar, S. (2016). Microstructural characterization of dissimilar stainless-steel welds. *Journal of Materials Engineering and Performance*, 25(7), 2893–2902.
12. Deng, D., & Murakawa, H. (2008). Numerical simulation of welding distortion and residual stresses. *Computational Materials Science*, 43(2), 353–365.
13. Loto, C. A. (2013). Corrosion behavior of welded stainless steel in chloride environments. *Journal of Materials Engineering and Performance*, 22(9), 2615–2623.

Wang, X., Liu, Y., & Li, J. (2018). Microstructure and corrosion behavior of welded stainless steels. *Corrosion Science*,